Journal of Pharmaceutical and Biomedical Analysis 52 (2010) 332–344

Contents lists available at ScienceDirect

Journal of Pharmaceutical and Biomedical Analysis

journal homepage: www.elsevier.com/locate/jpba

Characterization of degradation products of amorphous and polymorphic forms of clopidogrel bisulphate under solid state stress conditions

Dhara K. Raijada, Bhagwat Prasad, Amrit Paudel, Ravi P. Shah, Saranjit Singh*

Department of Pharmaceutical Analysis, National Institute of Pharmaceutical Education and Research (NIPER), Sector 67, S.A.S. Nagar, Mohali 160062, Punjab, India

ARTICLE INFO

Article history:
Received 20 April 2009
Accepted 2 May 2009
Available online 12 May 2009

Keywords:
Clopidogrel bisulphate
Solid state degradation
Stress studies
LC–MS/TOF
LC–MS^n

ABSTRACT

The present study deals with the stress degradation studies on amorphous and polymorphic forms of clopidogrel bisulphate. The objective was to characterize the degradation products and postulate mechanism of decomposition of the drug under solid state stress conditions. For that, amorphous form, polymorph I and polymorph II of the drug were exposed to 40 °C/75% relative humidity (RH), with and without stressors for 3 months. The samples were analyzed by HPLC, and the relative extent of degradation as well as nature of decomposition was compared among three solid forms. In total, eight degradation products were observed under various stress conditions. The structures of all of them were elucidated using LC–MS/TOF and LC–MS^n studies. While one matched the known hydrolytic decomposition product of the drug in solution, seven others were new. The postulated degradation pathway and mechanism of decomposition are discussed.

1. Introduction

Due to diverse solid forms (amorphous, pseudopolymorphs, polymorphs), a drug can show differences in its pharmaceutical properties. Therefore, it is important to characterize and control solid state properties much early during the product development. The choice of a solid form is also associated with regulatory and intellectual property issues [1]. Among all the pharmaceutical properties influenced by solid forms of the drug, solubility and bioavailability are the most studied [2–4]. However, very less has been reported regarding chemical reactivity or stability of solid forms of drugs, even though substantial advances have taken place in the knowledge of chemical and physical factors governing solid state reactions of molecular crystals [5,6].

A few literature examples are available revealing importance of stability in solid state. These include (i) pronounced difference in the reactivities of α and β forms of aztreonam [7], (ii) formation of different products in solution and solid state in case of tolerastat [8], and (iii) formation of oxidative degradation products of forms I and V of hydrocortisone 21-*tert*-butyl acetate (HTBA), while forms II–IV were resistant to air oxidation [9].

Considering these examples, the present study was carried out to explore the differences in degradation behaviour of various solid forms of clopidogrel bisulphate through solid state stress studies. Clopidogrel bisulphate (Fig. 1) is an antiplatelet drug, which acts by selective and irreversible inhibition of ADP-induced platelet aggregation. The drug is available in the market as oral solid dosage form. Six different polymorphs are known for the drug, but only two (polymorph I and polymorph II) are used commercially [10]. Both of these forms have almost similar bioavailability [11]. The amorphous form of the drug has also been tried for commercial use [12,13]. In the literature, a few reports exist on the decomposition behaviour of drug in solution [14–17], but no report exists on the degradation behaviour of its solid forms.

The studies were carried out in the following steps: (i) forced degradation of amorphous form and polymorph I and polymorph II of clopidogrel bisulphate under a variety of solid state stress conditions, (ii) development of HPLC method to separate degradation products from the drug, (iii) conduct of LC–MS/TOF and MS^n studies to establish fragmentation profiles of the drug and degradation products, (iv) structure elucidation of degradation products through comparative study of mass data, and (v) establishment of degradation pathway and mechanism of decomposition of the drug in solid state.

2. Experimental

2.1. Chemicals and reagents

Pure polymorphs (I and II) of clopidogrel bisulphate were obtained as gratis samples from Ind-Swift Laboratories Ltd. (S.A.S. Nagar, Punjab, India). The amorphous form was generated in-house from polymorph II. HPLC grade acetonitrile was purchased from J.T. Baker (Mexico City, Mexico, USA). Buffer salts and all other

* Corresponding author. Tel.: +91 172 2214682; fax: +91 172 2214692.
E-mail address: ssingh@niper.ac.in (S. Singh).

0731-7085/$ – see front matter © 2009 Elsevier B.V. All rights reserved.
doi:10.1016/j.jpba.2009.05.001

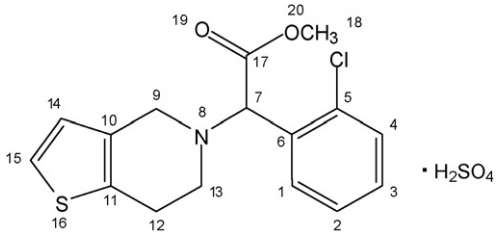

Fig. 1. Structure of clopidogrel bisulphate.

chemicals were of analytical reagent grade. Spectroscopic grade deuterated water (D_2O) and acetonitrile (CD_3CN) used in hydrogen deuterium exchange-MS (HDE-MS) experiments were procured from Sigma–Aldrich (St. Louis, MO, USA). Ultrapure water was obtained from ELGA water purification unit (Bucks, England).

2.2. Apparatus and equipment

HPLC analyses were performed on a 1200 series LC system from Agilent Technologies (Waldbronn, Germany) equipped with an on-line degasser (G1379A), high-pressure binary pump (G1312A), auto-injector (G1329A), thermostated column compartment (G1316A), and photodiode array detector (G1315B). For data processing and acquisition, Chemstation 01.03 software (Agilent Technologies) was used. Chromatographic separations were achieved on a C-8 column (250 mm × 4.6 mm i.d., particle size 5 μm, Supelco discovery Inc., Bellefonte, PA, USA). LC–MS/TOF studies were carried out on a system in which LC part consisted of 1100 series HPLC from Agilent Technologies (Waldbronn, Germany) and MS part consisted of MicrOTOF-Q spectrometer (Bruker Daltonics, Bremen, Germany). The LC part comprised of an on-line degasser (G1379A), binary pump (G131A), auto-injector (G1313A), column oven (G1316A) and diode-array detector (G1315B) was used. The system was controlled by Hyphenation Star (version 3.1) and MicrOTOF Control (version 2.0) software.

LC–MS^n studies were carried out using Accela™ (Thermo Electron Corporation, San Jose, USA) liquid chromatography system coupled to an LTQ XL™ linear ion trap mass spectrometer (Thermo Electron Corporation) via an electrospray interface. Instrument control and data collection were handled by Xcalibur software (Version 2.0.7 SP1, Thermo Fisher Scientific Inc., San Jose, USA).

Powder X-ray diffraction (PXRD) patterns were recorded at room temperature on Bruker's D8 advanced diffractometer (Karlsruhe, West Germany) Cu Kα radiation (λ = 1.54060 Å), obtained at 20 mA and 35 kV passing through nickel filter with divergent slit (0.5°), and receiving slit (1 mm). The diffractometer was equipped with a 2θ-compensating slit, which was calibrated with a silicon pellet. Data were processed using the DIFFRAC^{plus} EVA (ver. 9.0) diffraction software. The scans were run from 3° to 40° 2θ, increasing at a step size of 0.05° with a counting time of 5 s for each step.

Solid state stress studies were carried out in dark and light stability chambers (KBF 720 and KBWF 240, respectively) (WTC Binder, Tuttlingen, Germany). pH/Ion analyzer (MA 235, Mettler Toledo, Schwerzenbach, Switzerland) was used to adjust and check the pH of buffers and other solutions. Other equipments used were sonicator (model 3210, Branson Ultrasonics Corporation, Connecticut, USA), analytical balance (Mettler Toledo, Schwerzenbach, Switzerland), auto-pipettes (Eppendorf, Hamburg, Germany) and rotavapor (Buchi Rotavapor R-114, Switzerland).

2.3. Generation of solid state stress samples

For pH stress studies, 10 mg each of amorphous form, polymorph I and polymorph II were accurately weighed into 15 ml vials. 20 mg each of oxalic acid and sodium carbonate were added to these vials to create acidic and alkaline pH microenvironment, respectively. The contents were mixed using a glass capillary. Separate sets were prepared without any additive to allow for study at inherent pH of the drug. Sufficient number of samples was prepared to allow for withdrawal of replicates after 1 and 3 months for HPLC and LC–MS analyses (Table 1). The samples in open vials were charged to dark and light stability chambers set at 40 °C/75% relative humidity (RH).

For oxidative stress studies in solid state, all the three solid forms of the drug were taken in glass ampoules with long neck, and oxygen gas was purged for 5 min. Ampoules were then immediately sealed and charged into stability chamber set at 40 °C/75% RH. The samples were withdrawn at the end of 1 and 3 months, and analyzed for physical and chemical changes.

2.4. Development and validation of a stability-indicating HPLC method

In order to achieve separation among the degradation products and the drug, different HPLC parameters like, type, capacity and pH of buffers; ratio of buffer:organic modifier; flow rate; isocratic/gradient mode, and detection wavelength were optimized. The developed method was validated with respect to linearity, precision (intra-day, inter-day and intermediate precision), accuracy and specificity. To establish linearity and range, a stock solution containing 2 mg/ml drug in ACN (acetonitrile) was serially diluted to yield solutions in the concentration range of 100–1000 μg/ml. The solutions were prepared in triplicate and analyzed by injecting 4 μl into HPLC. The intra- and inter-day precision were established by analyzing 200, 400 and 600 μg/ml drug solutions three times on the same day and on three consecutive days, respectively. To determine intermediate precision, the whole experiment was conducted on two different columns. Accuracy was determined by spiking a mixture of stressed samples with the above given three known concentrations of the drug in triplicate and then determining the percent recovery of the added drug. Specificity of the method was

Table 1
Generation of solid state stress samples.

pH effect	Additive	pH[a]	Replicate sample numbers				
			Dark chamber study			Light chamber study	
			HPLC analysis		LC–MS	HPLC analysis	LC–MS
			1 month	3 months	3 months	1.2×10^6 lx h fluorescent light and 200 Wh/m^2 UV light	
Without additive	–	2.7	3	3	1	3	1
Acidic	Oxalic acid	1.3	3	3	1	3	1
Alkali	Sodium carbonate	10.1	3	3	1	3	1

[a] pH of the microenvironment was determined by the method given by Serajuddin et al. [18].

Table 2
Parameters of the developed ESI positive MS/TOF and MS^n methods.

MS/TOF parameters	End plate offset (V)	−500
	Capillary (V)	−4,500
	Nebuliser (Bar)	1.2
	Dry gas (l/min)	6.0
	Dry temperature (°C)	200
	Funnel 1 RF (Vpp)	150
	Funnel 2 RF (Vpp)	190
	ISCID energy (eV)	6.0
	Hexapole RF (Vpp)	200
	Ion energy	0.0
	Low mass (*m/z*)	200
	Collision energy (eV/z)	7.0–20.0[a]
	Transfer time (μs)	38.0–80.0[a]
	Collision RF (Vpp)	220–240[a]
	Pre-pulse storage (μs)	4.0–6.0[a]
	Detector voltage (V)	−1,200
MS^n parameters	Spray voltage (kV)	4.75
	Capillary temperature (°C)	250
	Vaporizer temperature (°C)	200
	Helium gas flow rate (ml/min)	0.5
	Scan rate for product ions (amu/s)	11,000

[a] Parameters were varied according to the nature of drug and degradation products to get optimum fragmentation.

established by determining purity parameters using a PDA detector.

2.5. HPLC analyses of solid state stressed samples

The samples collected after 1 and 3 months were evaluated for physical and chemical changes. Physical changes were observed visually. For chemical analyses, 3 ml of ACN:water (50:50) was added to each glass vial, followed by sonication for 3–4 min in an ultrasonic bath. The contents were transferred to a 10-ml volumetric flask and the volume was made up with ACN:water (50:50). In each case, 4 μl of the resultant solution was injected into an HPLC system ($n = 3$). In each condition, percent drug remaining was calculated, and used for comparison of degradation/rate of decomposition among various solid forms.

2.6. Mass fragmentation studies on clopidogrel

First, *in silico* studies were carried out to predict fragmentation behaviour of the drug using Frontier software (Version 5.1.0.1, Thermo Electron Corporation). To record mass spectra, MS^n and MS/TOF parameters were optimized to get the best ionization, without compromising on intensity (Table 2). For MS^n studies, 500 ng/ml solution of the drug was directly injected at a flow rate of 10 μl/min and the MS parameters were optimized to get best possible fragmentation with acceptable sensitivity. The response of the LC–MS/TOF system for high resolution mass spectrometric (HR-MS) studies was optimized using a 10-μg/ml drug solution, which was injected directly at a flow rate of 3 μl/min. HDE-MS experiments were carried on the drug solution prepared in D_2O:CD_3CN (50:50).

2.7. LC–MS/TOF and LC–MS^n studies and characterization of degradation products

The developed gradient LC method was transferred to LC–MS/TOF by replacing phosphate buffer with water (pH adjusted to 2.75 with formic acid). For structure elucidation, samples with maximum degradation were subjected to LC–MS studies. The mass parameters, such as collision energy, transfer time, collision RF and pre-pulse storage were varied to identify molecular ion peaks of degradation products first, and then to optimize their fragmentation. The degradation products were also subjected to LC–MS^n analyses to determine their fragmentation pathways.

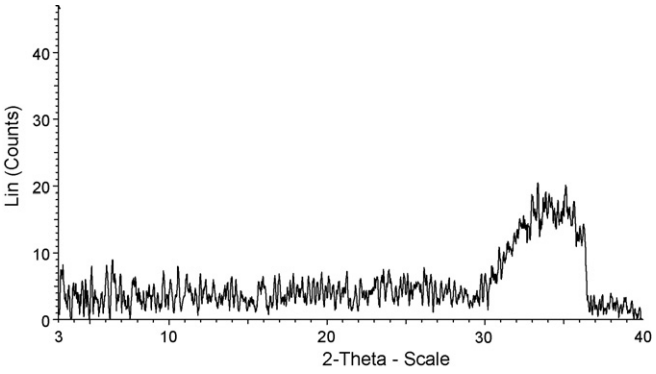

Fig. 2. XRD pattern of amorphous form of clopidogrel bisulphate.

3. Results and discussion

3.1. Generation of amorphous form

Several methods including freeze drying, spray drying, rapid precipitation, quench cooling, solvent evaporation, *etc.* have been reported for the generation of amorphous form of clopidogrel bisulphate [11,19,20]. The solvent evaporation method involving addition of ethanol [12] resulted in a physically stable amorphous form, which showed a halo XRD pattern (Fig. 2).

3.2. Stability-indicating HPLC method

An optimum resolution among the drug and its degradation products was obtained using the following HPLC conditions: mobile phase, ACN (A) and KH_2PO_4 buffer (10 mM, pH 2.75) (B); gradient, T_{min}/A:B (v/v); $T_{0.01-2}$/2:98 (v/v), T_{5-15}/20:80 (v/v), T_{35}/80:20 (v/v), T_{40-48}/2:98 (v/v); flow rate, 1 ml/min; detection wavelength, 235 nm; and injection volume, 4 μl. Fig. 3 depicts the stability-indicating nature of the developed method. The degradation products were encoded DP-1 to DP-8, according to their order of elution in the chromatogram.

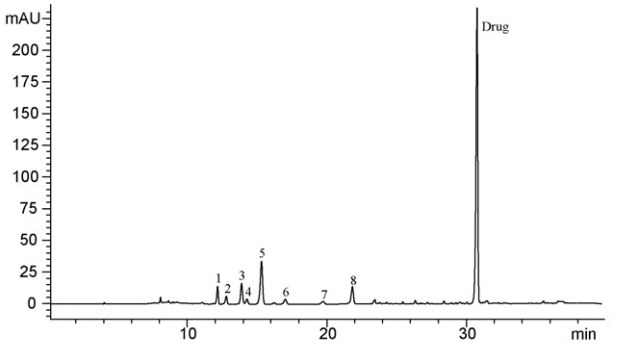

DP	1	2	3	4	5	6	7	8
Condition	Al	N, Al	N*, Al	N	A ,N, Al	N	N	Al
Solid form	Am,P1,P2	Am,P1,P2	Am,P1,P2	Am	Am,P1,P2	Am	Am	Am,P1,P2

Fig. 3. Chromatogram showing separation of degradation products formed in different solid forms under solid state stress conditions [DP-degradation product, A-acidic condition, Al-alkaline condition, N-neutral condition (without stressor), P1-polymorph I, P2-polymorph II, and Am-amorphous form]. *Only amorphous form leads to formation of DP-3 under neutral condition.

Table 3
Data of clopidogrel bisulphate from linearity studies.

Concentration (μg/ml)	Peak area 1	Peak area 2	Peak area 3	Average peak area	±S.D.	R.S.D. (%)
100	470.3	469.5	471.5	470.4	1.00	0.21
200	1011.5	1009.6	1008.1	1009.7	1.70	0.16
400	2032.7	2030.6	2033.4	2032.2	1.45	0.07
600	3097.6	3100.1	3095.1	3097.6	2.50	0.08
800	4183.9	4175.9	4175.2	4178.3	4.83	0.11
1000	5270.9	5264.9	5279.4	5271.7	7.28	0.13

Table 4
Intra- and inter-day precision studies.

Concentration (μg/ml)	Intra-day precision, measured concentration ±S.D. (μg/ml), R.S.D. (%)	Inter-day precision, measured concentration ±S.D. (μg/ml), R.S.D. (%)
200	200.7398 ± 0.656, 0.32	198.9482 ± 2.626, 1.319
400	400.6709 ± 2.347, 0.586	399.9818 ± 6.646, 1.661
600	600.6584 ± 3.510, 0.584	601.2848 ± 7.598, 1.263

Table 5
Recovery data for clopidogrel bisulphate spiked into a mixture of stressed samples.

Spiked concentration (μg/ml)	Calculated spiked concentration (μg/ml) ± S.D., R.S.D. (%)	Recovery (%)
200	199.6748 ± 1.397, 0.699	99.83
400	401.9865 ± 2.172, 0.540	100.49
600	600.4705 ± 2.000, 0.333	100.07

3.3. Validation of the method

The system suitability results for both resolution and relative retention times were well within the limits. A linear response was obtained in the concentration range of 100–1000 μg/ml (R^2 = 0.999). The linearity data in Table 3 showed that percent R.S.D. for each concentration was <0.5%. The percent R.S.D. for intra- and inter-day precision studies at three different concentrations, *viz.*, 200, 400 and 600 μg/ml were less than 1% and 2%, respectively (Table 4). Also, good recoveries were obtained when a mixture of stressed samples was spiked with the drug at the above given three concentrations (mean recovery = 100.13%, Table 5). As shown in Fig. 3, the method had sufficient specificity, as it could separate drug and its major degradation products formed at an area percent of >1% with a resolution factor of >1.5 for each peak. Specificity was proved through peak purity data obtained using a PDA detector (Table 6).

3.4. Physical and chemical stability of various forms of drug under solid state stress conditions

3.4.1. Physical changes

The physical changes observed after storage of the three solid forms of clopidogrel bisulphate in the absence and the presence of acid and alkali stressors, are summarised in Table 7. The table clearly indicates that all the samples became damp or sticky at 40 °C/75% RH. In particular, the amorphous form gained more moisture due to its severe hygroscopic nature. Also, all the three forms of the drug showed significant colour change under alkali stress condition. The amorphous form was discoloured even in samples without the stressor. There was no evident influence of light or oxidative stress.

Table 6
Peak purity data of drug and degradation products.

Drug/degradation product	Peak purity index
DP-1	0.99918
DP-2	0.99901
DP-3	0.99916
DP-4	0.99858
DP-5	0.99923
DP-6	0.99899
DP-7	0.99981
DP-8	0.99911
Drug	0.99991

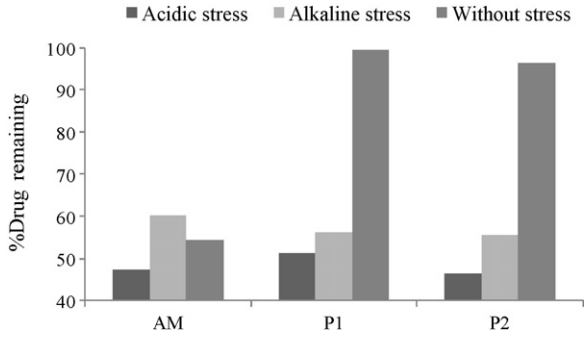

Fig. 4. Chemical decomposition in the presence and absence of acid and alkali stressors on storage at 40 °C/75% RH for 3 months.

3.4.2. Chemical degradation

Fig. 4 shows the chemical changes (% drug remaining) observed for various solid forms on storage for 3 months at 40 °C/75% RH in the absence and the presence of acid and alkali stressors. As evident, the extent of degradation among the three solid forms was almost similar under acidic and alkaline microenvironment. However, the amorphous form showed ~40% more degradation than polymorphic forms in samples without stressors. As shown in Fig. 3, the three solid forms had somewhat different nature of degradation. In samples without stressor (neutral condition), the amorphous form resulted in almost six degradation products, *viz.*, DP-2 to DP-7, while both polymorphic forms resulted in only two products, DP-2 and DP-5. There was no difference in the nature of degradation among the three forms under acid and alkali microenvironment. The solid

Table 7
Physical changes in solid state stressed samples on exposure in dark (3 months) and light stability chambers (6 d).

Samples	Acid stress		Alkali stress		Without stressor		Oxygen stress	
	Dark	Light	Dark	Light	Dark	Light	Dark	Light
Amorphous	Sticky mass	Sticky mass	Brown, sticky granules	Creamish, sticky granules	Dark brown, sticky paste	Creamish, sticky mass	NC	NC
Polymorph I	Sticky mass	NC	Brown, slight sticky granules	Slight creamish	Damp powder	NC	NC	NC
Polymorph II	Sticky mass	NC	Brown, slight sticky granules	Slight creamish	Damp powder	NC	NC	NC

NC: no change.

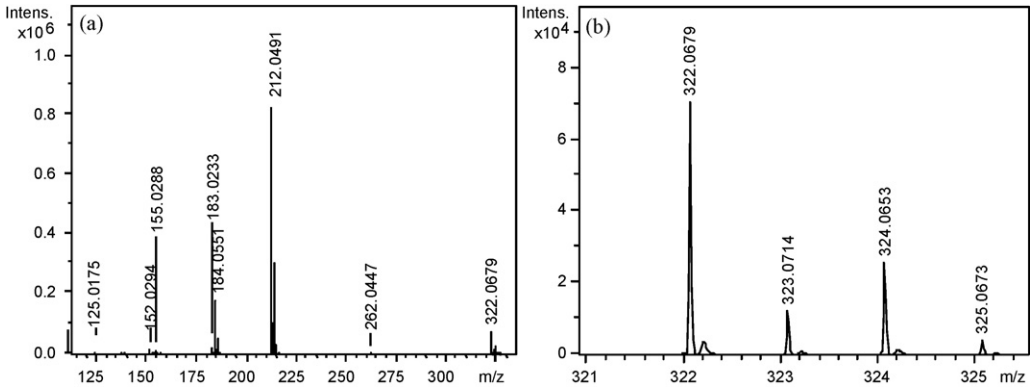

Fig. 5. Mass spectrum of clopidogrel (a) and isotopic pattern of molecular ion peak of drug (b).

Table 8
MS/TOF data of clopidogrel and its fragments.

Experimental mass	Theoretical mass	Error (ppm)	H/D exchange	Number of labile hydrogens	Number of nitrogens	Molecular formula (RDBs)	Isotopic pattern[a]	
							Experimental	Theoretical
322.0679	322.0663	4.96	323	1	Odd	$C_{16}H_{17}NO_2SCl$ (8.5)	100:17:37	100:17:32
262.0447	262.0452	−1.90	262	0	Odd	$C_{14}H_{13}NSCl$ (8.5)	100:17:37	100:15:32
212.0491	212.0473	8.48	213	1	Odd	$C_{10}H_{11}NO_2Cl$ (5.5)	100:12:37	100:11:32
184.0551	184.0524	14.66	185	1	Odd	$C_9H_{11}NOCl$ (4.5)	100:8:30	100:10:32
183.0233	183.0207	14.20	183	0	Even/zero	$C_9H_8O_2Cl$ (5.5)	100:9:32	100:10:32
155.0288	155.0258	19.35	155	0	Even/zero	C_8H_8OCl (4.5)	100:11:33	100:9:32
152.0294	152.0262	21.04	152	0	Odd	C_8H_7NCl (5.5)	100:7:28	100:9:32
125.0175	125.0153	17.59	125	0	Even/zero	C_7H_6Cl (4.5)	100:7:28	100:8:32

[a] Isotopic ratio is presented as $[M+H]^+$:$[M+H+1]^+$:$[M+H+2]^+$.

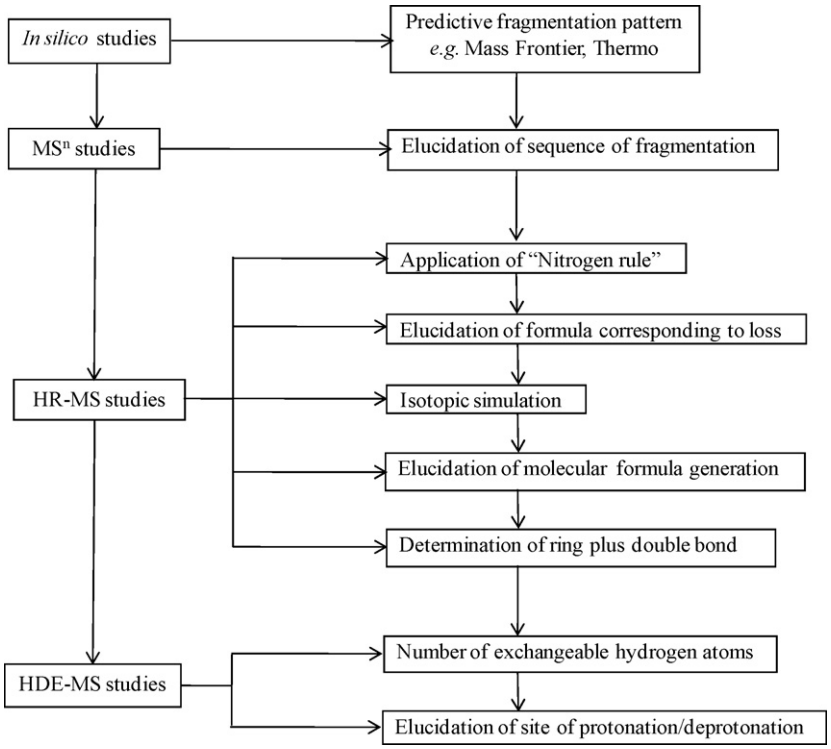

Fig. 6. Generic strategy for postulation of mass fragmentation pattern.

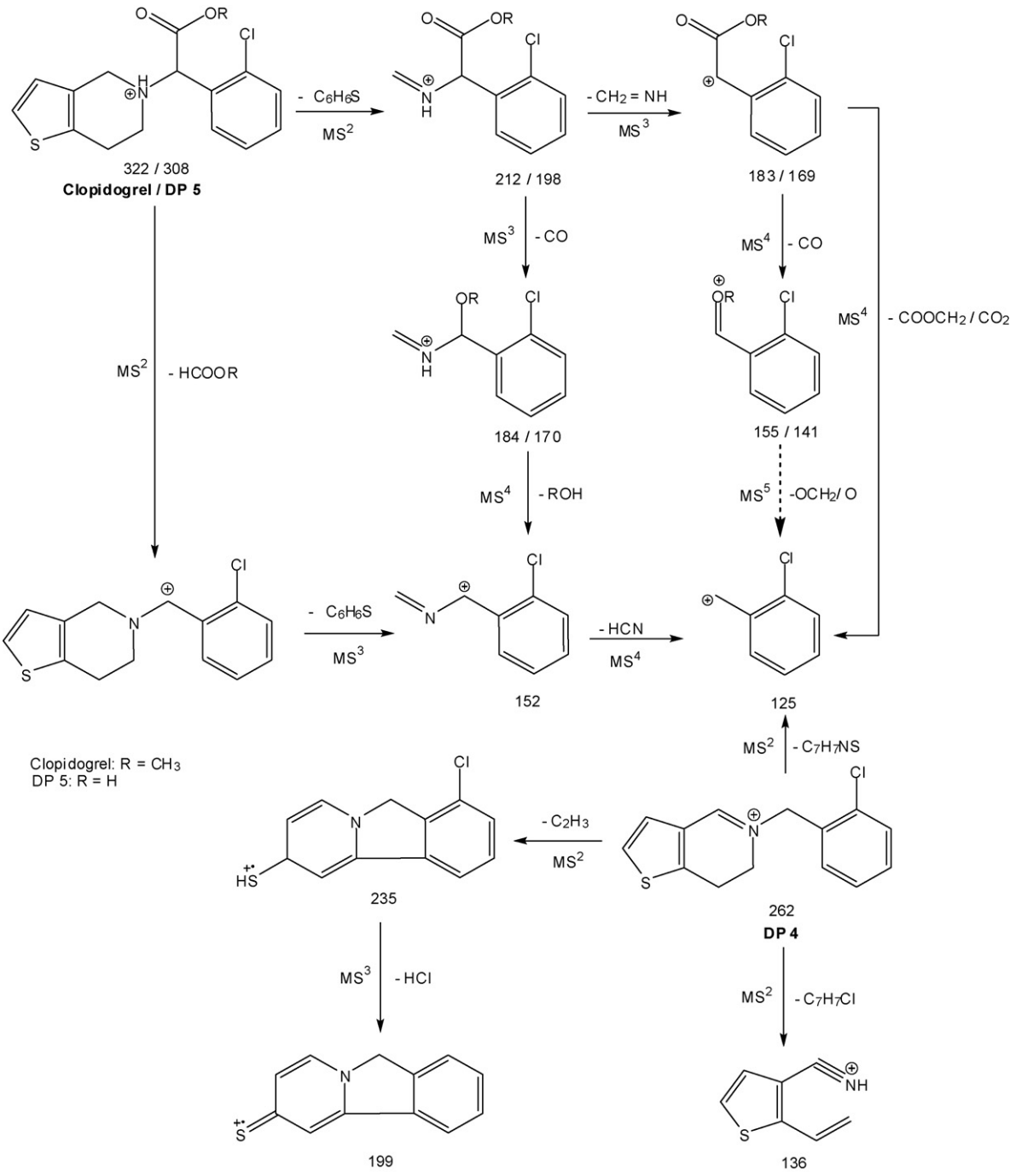

Scheme 1. Fragmentation profiles of clopidogrel, DP-5 and DP-4.

forms were also stable chemically to oxidative and photolytic conditions.

3.5. HR-MS, HDE-MS and MS^n studies on the drug

The drug showed good fragmentation in ESI positive mode (Fig. 5). Accurate mass data, HDE-MS results, molecular formulae, and isotopic ratios for all the fragments are compiled in Table 8. The fragmentation profile was delineated using these data, supplemented by elucidation of the sequence of fragmentation by MS^n studies. The general strategy adopted for the same is outlined in Fig. 6.

It is evident from Fig. 5a that the molecular ion peak $[M+H]^+$ of clopidogrel had m/z of 322 and the fragments appeared at m/z 262, 212, 184, 183, 155, 152 and 125. An almost similar mass fragmentation was observed by Danikiewiczl and Swist [21], except a low abundant ion of m/z 262, which was additionally observed in our study. The isotopic pattern, as shown in Fig. 5b, had the expected $[M+H+2]^+$ isotopic peak due to the presence of chlorine in the drug structure. Similar isotopic pattern was observed for all the fragments, highlighting that the portion of drug molecule containing chlorine was unaffected by the mass ionization.

The fragmentation pathway for the drug, incorporating postulations by Danikiewiczl and Swist [21] and additional elements from our study, is outlined in Scheme 1. The additional fragment of m/z 262 emerged at low collision energies from the loss of methyl formate moiety from the drug. The same was supported by accurate

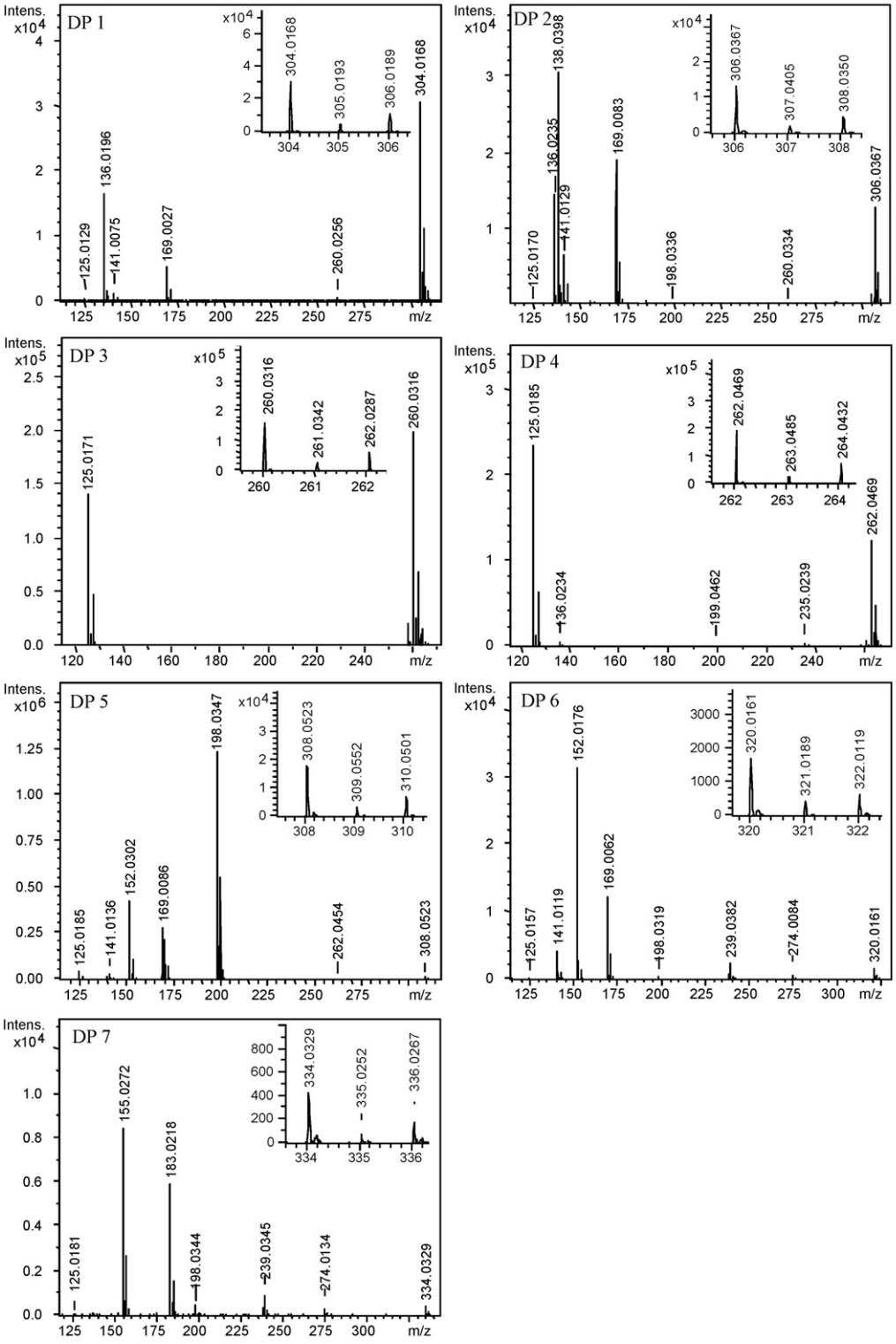

Fig. 7. Mass spectra of DP 1 to DP 7. The isotopic pattern of molecular ion peaks are shown in insets.

mass analyses and HDE studies (Table 8). A different structure of the fragment ion of *m*/*z* 152, than proposed by Danikiewiczl and Swist [21], is shown in Scheme 1. The reported structure of the fragment had an exchangeable hydrogen, while HDE study at our end showed absence of the same (Table 8).

It was formed from a fragment of *m*/*z* 262 in MS^3 in minor form and from *m*/*z* 184 in MS^4 as a major fragment. The MS^4 result in our study postulates that the preferred route of formation of *m*/*z* 125 was from *m*/*z* 183 through the loss of $-C_2H_2O_2$ moiety, than the pathway *m*/*z* 183 → 155 → 125.

3.6. LC–MS studies for characterization of degradation products

The LC–MS/TOF spectra of degradation products, along with isotopic patterns for molecular ion peaks, are shown in Figs. 7 and 8. Table 9 lists the theoretical and observed accurate mass values,

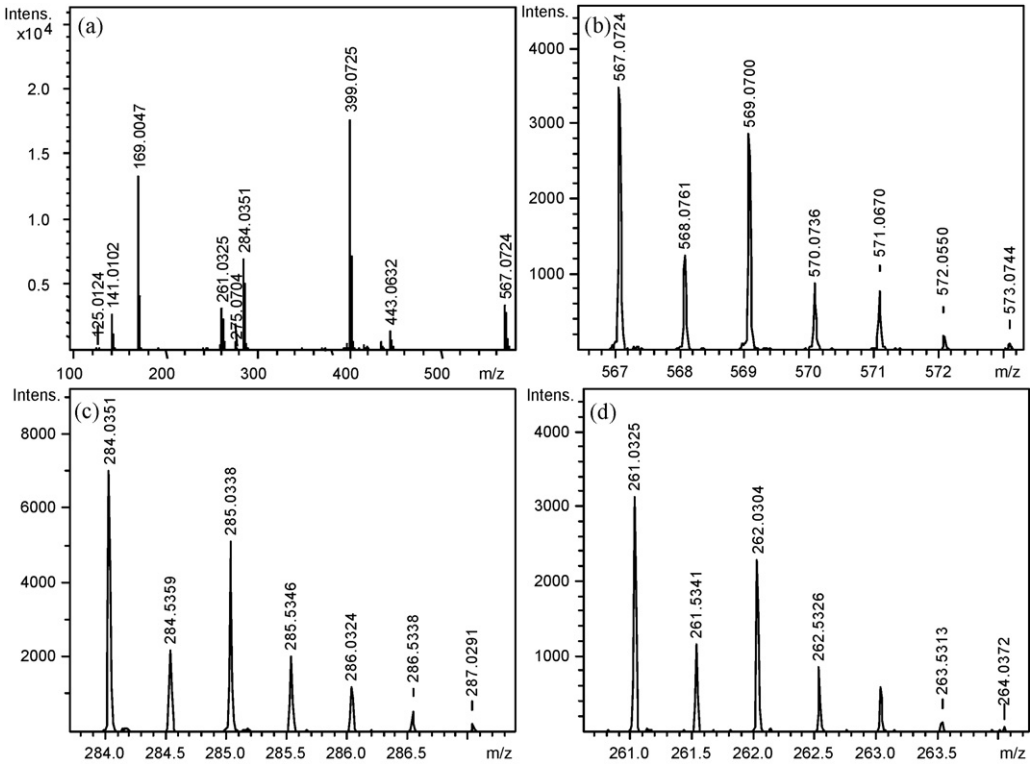

Fig. 8. Mass spectrum of DP-8 (a), isotopic pattern of molecular ion peak of singly charged DP-8 (b), isotopic pattern of molecular ion peak of doubly charged DP-8 (c), and isotopic pattern of peak of doubly charged fragment of DP-8 (d).

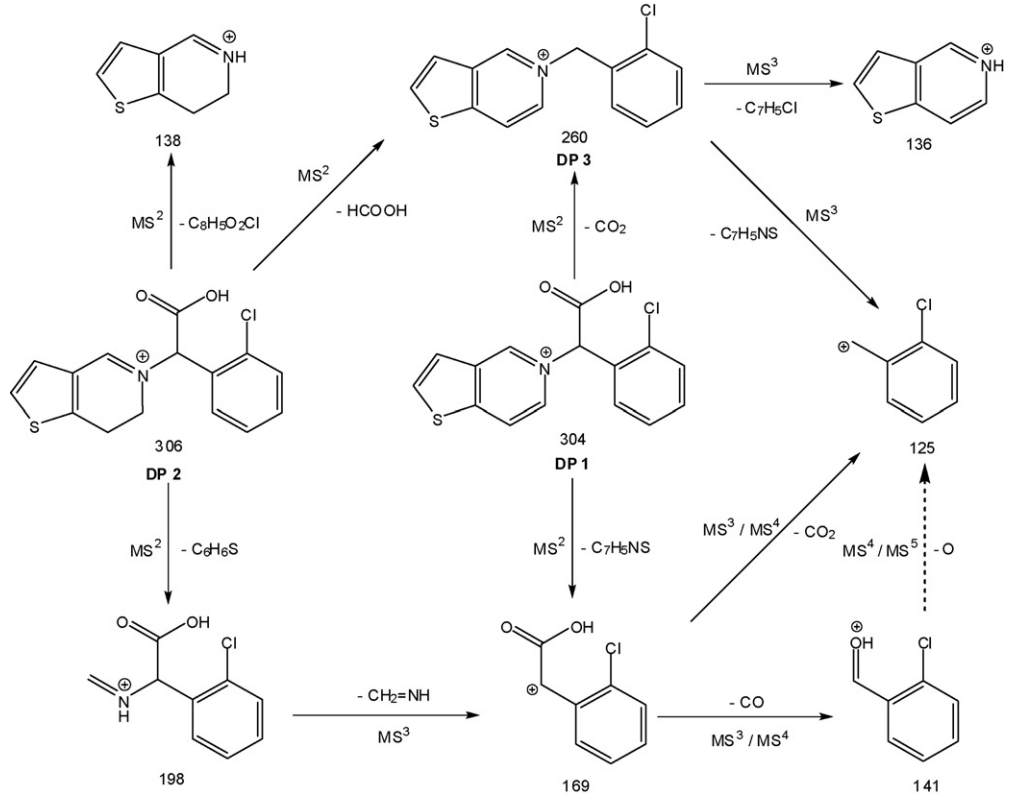

Scheme 2. Fragmentation profiles of DP-1, DP-2 and DP-3.

Table 9
LC–MS/TOF data of degradation products and their fragments.

Degradation products	Experimental mass	Theoretical mass	Error (ppm)	Number of nitrogens	Molecular formula (RDB)	Isotopic pattern	
						Experimental	Theoretical
DP-1	304.0168	304.0194	−8.55	Odd	$C_{15}H_{11}NO_2SCl$ (10.5)	100:15:37	100:16:32
	260.0256	260.0295	−14.99	Odd	$C_{14}H_{11}NSCl$ (9.5)	100:16:39	100:15:32
	169.0027	169.0051	−14.20	Even/zero	$C_8H_6O_2Cl$ (5.5)	100:9:32	100:9:32
	141.0075	141.0102	−19.14	Even/zero	C_7H_6OCl (4.5)	100:7:29	100:8:32
	136.0196	136.0215	−13.96	Odd	C_7H_6NS (5.5)	100:9:5	100:8:5
	125.0129	125.0153	−19.19	Even/zero	C_7H_6Cl (4.5)	100:8:31	100:8:32
DP-2	306.0367	306.035	5.55	Odd	$C_{15}H_{13}NO_2SCl$ (9.5)	100:15:36	100:16:32
	260.0334	260.0295	14.99	Odd	$C_{14}H_{11}NSCl$ (9.5)	100:15:38	100:15:32
	198.0336	198.0316	10.09	Odd	$C_9H_9NO_2Cl$ (5.5)	100:12:38	100:10:32
	169.0083	169.0051	18.93	Even/zero	$C_8H_6O_2Cl$ (5.5)	100:11:27	100:9:32
	141.0129	141.0102	19.14	Even/zero	C_7H_6OCl (4.5)	100:10:37	100:8:32
	136.0235	136.0215	14.70	Odd	C_7H_6NS (5.5)	100:9:94[a]	100:8:5
	138.0398	138.0372	18.83	Odd	C_7H_8NS (4.5)	100:11:5[a]	100:8:5
	125.017	125.0153	13.59	Even/zero	C_7H_6Cl (4.5)	100:10:38	100:8:32
DP-3	260.0316	260.0295	8.07	Odd	$C_{14}H_{11}NSCl$ (9.5)	100:18:41	100:15:32
	125.0171	125.0153	14.39	Even/zero	C_7H_6Cl (4.5)	100:7:31	100:8:32
DP-4	262.0469	262.0452	6.48	Odd	$C_{14}H_{13}NSCl$ (8.5)	100:13:38	100:15:32
	235.0239	235.0217	9.36	Even/zero[b]	$C_{12}H_{10}NSCl$ (8.0)	100:15:37	100:13:32
	199.0462	199.045	6.02	Even/zero[b]	$C_{12}H_9NS$ (9.0)	100:16:6	100:13:5
	136.0234	136.0215	13.96	Odd	C_7H_6NS (5.5)	100:9:7	100:8:5
	125.0185	125.0153	25.59	Even/zero	C_7H_6Cl (4.5)	100:6:27	100:8:32
DP-5	308.0528	308.0507	6.81	Odd	$C_{15}H_{15}NO_2SCl$ (8.5)	100:18:39	100:17:32
	262.0454	262.0452	0.76	Odd	$C_{14}H_{13}NSCl$ (8.5)	100:19:37	100:15:32
	198.0347	198.0316	15.65	Odd	$C_9H_9NO_2Cl$ (5.5)	100:14:37	100:10:32
	170.0411	170.0367	25.87	Odd	C_8H_9NOCl (4.5)	100:37:33[a]	100:9:32
	169.0086	169.0051	20.70	Even/zero	$C_8H_6O_2Cl$ (5.5)	100:71:26[a]	100:9:32
	152.0302	152.0262	26.31	Odd	C_8H_7NCl (5.5)	100:7:26	100:9:32
	141.0136	141.0102	24.11	Even/zero	C_7H_6OCl (4.5)	100:15:24	100:8:32
	125.0185	125.0153	25.59	Even/zero	C_7H_6Cl (4.5)	100:7:30	100:8:32
DP-6	320.0161	320.0143	5.62	Odd	$C_{15}H_{11}NO_3SCl$ (10.5)	100:20:37	100:16:32
	274.0084	274.0088	−1.45	Odd	$C_{14}H_9NOSCl$ (10.5)	100:17:37	100:15:32
	239.0382	239.0399	−7.11	Even/zero[b]	$C_{14}H_9NOS$ (11.0)	100:16:6	100:15:5
	198.0319	198.0316	1.51	Odd	$C_9H_9NO_2Cl$ (5.5)	100:12:36	100:10:32
	169.0062	169.0051	6.50	Even/zero	$C_8H_6O_2Cl$ (5.5)	100:8:30	100:10:32
	152.0176	152.0165	7.23	Odd	C_7H_6NOS (5.5)	100:9:5	100:8:5
	141.0119	141.0102	12.05	Even/zero	C_7H_6OCl (4.5)	100:7:28	100:8:32
	125.0157	125.0153	3.19	Even/zero	C_7H_6Cl (4.5)	100:7:32	100:8:32
DP-7	334.0329	334.0299	8.98	Odd	$C_{16}H_{13}NO_3SCl$ (10.5)	100:17:41	100:17:32
	274.0134	274.0088	16.78	Odd	$C_{14}H_9NOSCl$ (10.5)	100:22:36	100:15:32
	239.0345	239.0399	−22.59	Even/zero[b]	$C_{14}H_9NOS$ (11.0)	100:22:8	100:15:5
	198.0344	198.0316	14.13	Odd	$C_9H_9NO_2Cl$ (5.5)	100:8:42	100:10:32
	183.0218	183.0207	6.01	Even/zero	$C_9H_8O_2Cl$ (5.5)	100:10:27	100:10:32
	155.0272	155.0258	9.03	Even/zero	C_8H_8OCl (4.5)	100:11:32	100:9:32
	152.0147	152.0165	−11.84	Odd	C_7H_6NOS (5.5)	100:8:5	100:8:5
	125.0181	125.0153	22.31	Even/zero	C_7H_6Cl (4.5)	100:7:32	100:8:32
DP-8	567.0724	567.0729	−0.88	Even/zero	$C_{29}H_{25}N_2O_2S_2Cl_2$ (17.5)	100:36:78	100:31:64
	443.0632	443.0649	−3.83	Even/zero	$C_{22}H_{20}N_2O_2S_2Cl$ (13.5)	100:28:37	100:24:32
	399.0725	399.0751	−6.51	Even/zero	$C_{21}H_{20}N_2S_2Cl$ (12.5)	100:27:40	100:23:32
	284.0351	284.0401	−17.60	Even/zero	$C_{29}H_{26}N_2O_2S_2Cl_2$ (17)	100:33:69	100:31:64
	275.0704	275.0671	11.99	Even/zero	$C_{14}H_{15}N_2S_2$ (8.5)	100:15:9	100:15:9
	261.0325	261.0374	−18.57	Even/zero	$C_{28}H_{24}N_2S_2Cl_2$ (17)	100:32:77	100:30:64
	169.0047	169.0051	−2.36	Even/zero	$C_8H_6O_2Cl$ (5.5)	100:10:31	100:9:32
	141.0102	141.0102	0	Even/zero	C_7H_6OCl (4.5)	100:9:35	100:8:32
	125.0124	125.0153	−23.19	Even/zero	C_7H_6Cl (4.5)	100:8:33	100:8:32

[a] Isotopic ratios were not in congruence with theoretical, as the $[M+H]^+$ peaks of *m/z* 170, 138 were merged with $[M+H+1]^+$ peak and $[M+H+2]^+$ peak of *m/z* 169 and *m/z* 136, respectively.
[b] Nitrogen rule was not followed because the fragments were radical cations.

along with error in ppm, molecular formulae, number of nitrogens, and isotopic ratios for all the degradation products and their fragments. As evident from mass spectra and isotopic patterns in Fig. 7 and from data in Table 9, all the degradation products (DP-1 to DP-7) had intense peaks of $[M+H+2]^+$ with abundance of ~32%, indicating the presence of chlorine atom. In all the cases, *m/z* values of molecular ion peaks were even numbered, revealing the presence of an odd number of nitrogen atoms in their structures. Based on this information, MS^n data, and strategy described in Fig. 6 (except HDE, but with additional comparison of fragmentation pattern with the drug), it was possible to propose the structures of degradation products and their fragmentation profiles. The same are shown in Schemes 1–4. The details are discussed below.

3.7. Structures and fragmentation pathways of degradation products

3.7.1. DP-5, m/z 308

DP-5 was the lone degradation product in acidic condition, while it was formed as a major and minor product under neutral and

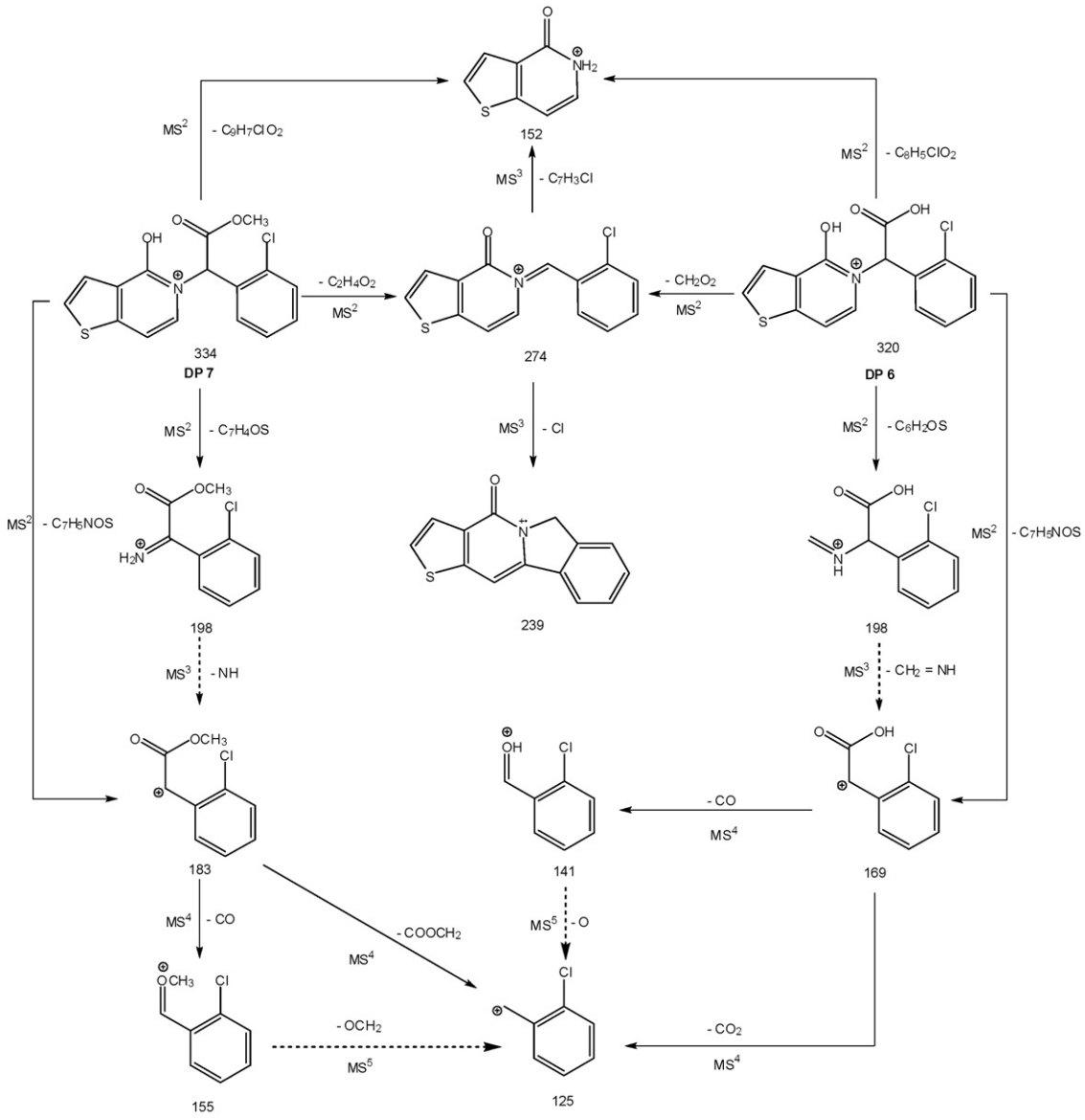

Scheme 3. Fragmentation profiles of DP-6 and DP-7.

alkaline conditions, respectively. The same was characterized to be clopidogrel acid, the only known hydrolytic product of the drug in solution [17]. The product is listed as impurity A in USP 2006 [22], and also reported as a major metabolite [23]. The observed mass of *m*/*z* 308 (Fig. 7) was same as the known product. Its mass fragmentation pattern is included in Scheme 1, and evidently is parallel/similar to the drug. As evident, its accurate mass was lower than the drug by ~14.0156 Da (*m*/*z* 322 → 308), and the same was the case for several other characteristic fragments, *viz.*, *m*/*z* 212 → 198, *m*/*z* 184 → 170, *m*/*z* 183 → 169 and *m*/*z* 155 → 141.

3.7.2. DP-2, m/z 306

DP-2 was formed as a major product under neutral condition and a minor product in alkali. Its molecular formula determined from its accurate mass value was $C_{15}H_{13}NO_2SCl$ (Table 9). It had a difference of exact mass of ~2.0157 Da than DP-5 as well as RDB value of 9.5 against 8.5 for the latter. This clearly indicated that DP-2 was a dehydrogenated product of DP-5. Similarity of fragments of *m*/*z* 198, 169, 141 and 125 with those of DP-5 indicated the presence of unchanged carboxy(2-chlorophenyl)methylium moiety. Three possibilities existed for the formation of a double bond in the remaining portion, *i.e.*, between N8 and C7, C12 and C13, or between N8 and C9 (Fig. 1). The double bond between C9 and N8 was considered as most favourable site for proton abstraction, as it could provide resonance stability by extended conjugation. The other fragments observed for DP-2 were of *m*/*z* 260, 138 and 136 (Scheme 2 and Fig. 7).

3.7.3. DP-1, m/z 304

The accurate mass of DP-1, a major degradation product under alkaline condition, helped in postulating molecular formula of $C_{15}H_{11}NO_2SCl$. Its mass was less by ~2.0157 Da than DP-2, and RDB value was 10.5 against 9.5 of DP-2. As shown in Scheme 2, the fragment of *m*/*z* 260 purportedly resulted from loss of CO_2, instead of loss of formic acid from DP-2 and DP-5. Again, the similarity of fragments of *m*/*z* 169, 141 and 125 to those of DP-2 and DP-5 confirmed the presence of an intact carboxy(2-chlorophenyl)methylium moiety. This clearly meant that there was an additional double bond in DP-1 than DP-2. The existence of dehydrogenation was predicted between N-8 and C-9 (Fig. 1), as it along with the one double bond between C-12 and C-13 could provide aromaticity and favour resonance stability of the structure. This was substan-

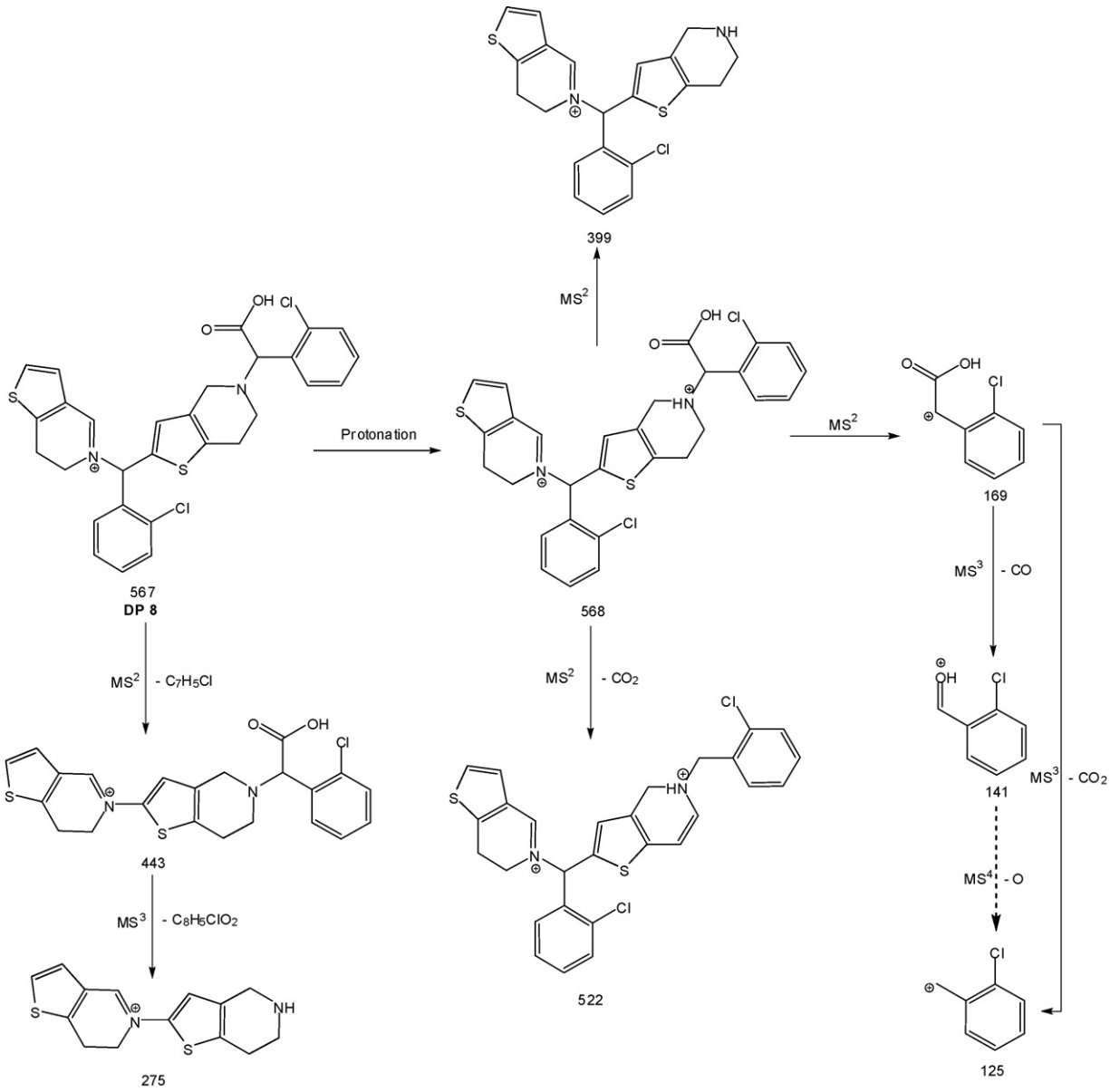

Scheme 4. Fragmentation profile of DP-8.

tiated by the absence of fragment of *m*/*z* 198 (Scheme 2), which otherwise was generated in DP-2 and DP-5 (Scheme 1). The formation of fragment of *m*/*z* 136 (Scheme 2) also confirmed the same.

3.7.4. DP-4, m/z 262

This product was formed under neutral condition only. Its molecular formula was determined to be $C_{14}H_{13}NSCl$. Based on the accurate mass (*m*/*z* 262.0469) and RDB value (8.5), it was considered to have a similar backbone structure as that of the fragment of the drug, with an accurate *m*/*z* of 262.0447 (Scheme 1, Table 8). It clearly meant that the product was devoid of methyl formate moiety present in the drug. Moreover, as shown in Fig. 7, the mass spectrum of DP-4 did not have fragments of *m*/*z* 183 and 155 pertaining to methyl ester moiety of the drug, and those of *m*/*z* 169 and 141 for the carboxylic acid group of DP-5. It is proposed that the loss of methyl formate moiety from the drug resulted in unsaturation between N8 and C9 (Fig. 1). Perhaps the double bond was formed initially between N8 and C7, and then it shifted to N8 and C9 to impart better conjugation stability.

As discussed earlier in Section 3.5, the fragment of the drug with *m*/*z* 262 on further MS^3 and MS^4 ionization resulted in the formation of a very low abundant ion of *m*/*z* 152 and a prominent ion of *m*/*z* 125 (Scheme 1). This was also true of DP-4 at low collision energies. However, at higher collision energies, an added fragmentation pathway of DP-4 was observed, as shown in Scheme 1. It involved formation of ions of *m*/*z* 235, 199 and 136 along with *m*/*z* 125. MS^n studies showed that the fragments of *m*/*z* 235, 136 and 125 were generated directly from DP-4, while ion of *m*/*z* 199 was formed from fragment of *m*/*z* 235.

3.7.5. DP-3, m/z 260

The accurate mass of this another major degradation product under alkaline condition helped in postulating molecular formula of $C_{14}H_{11}NSCl$. The difference of ~2.0157 Da and RDB value of 9.5 against 8.5 in DP-4 revealed that DP-3 was a further dehydrogenated product of DP-4. Similar to DP-4, the fragments of *m*/*z* 183

and 155 for methyl ester of the drug or *m/z* 169 and 141 for carboxylic acid of DP-5 were absent in DP-3 (Fig. 7), showing absence of either of the two moieties. The derived structure was similar to a fragment of DP-1, which had the same accurate mass and also common fragment ions of *m/z* 136 and 125 (Table 9). The fragmentation pathway of DP-3, merged with that of DP-1, is shown in Scheme 2.

3.7.6. DP-6, m/z 320, and DP-7, m/z 334

DP-6 and DP-7 were observed as minor products under neutral condition in amorphous form. Accurate masses of the two resulted in molecular formulae $C_{15}H_{11}NO_3SCl$ and $C_{16}H_{13}NO_3SCl$, respectively. The RDB value of 10.5 in both against 8.5 of the drug revealed the presence of unsaturated thieno-pyridine in their structures. The higher accurate mass of DP-6 by ~15.9949 Da than DP-1 (Table 9) revealed that it was hydroxylated product of the latter. The product DP-7 showed an accurate mass difference of ~14.0157 Da from DP-6, indicating that it had the methyl formate moiety against carboxylic acid in the structure of the latter, similar to the difference in structures of drug and DP-5. This was also substantiated by the presence of fragments of *m/z* 169 and 141 in DP-6 *versus* fragments of *m/z* 183 and 155 in DP-7 (Fig. 7). The common fragments of *m/z* 274, 239 and 152 underscored that the hydroxyl group was present in the thieno-pyridine moiety in both the products. The proposed fragmentation pathways for the two are combined in Scheme 3.

3.7.7. DP-8, m/z 567

This product, which was formed in alkaline condition, had molecular ion peak with an odd mass of *m/z* 567 (Fig. 8a), indicating even number of nitrogens in the structure. Also, the isotopic pattern of the peak (Fig. 8b) showed the presence of two chlorine atoms in the structure. Its *m/z* value of 567 and the presence of even number of nitrogens, including two chlorine atoms, gave all the indications of its being a dimeric product. The fragments of *m/z* 169 and 141 confirmed the presence of demethylated moiety of the drug in the structure (similar to DP-5); while fragment of *m/z* 399 revealed the presence of DP-4 moiety (*m/z* 262) at *ortho* to sulphur in the dimeric product. As shown in Fig. 8a, there was a peak of *m/z* 284, which was not assignable to any possible fragment of the product. Hence, it was attributed to $[M+2H]^{2+}$ doubly charged ion of 568 Da of the dimer. The same was substantiated even from the study of isotopic pattern (Fig. 8c), wherein $[M+2H+1]^{2+}$ and $[M+2H+2]^{2+}$ peaks at *m/z* 284.5 and 285.0, respectively, were clearly evident. Similarly, another fragment in Fig. 8a with a *m/z* of 261 was also purported to be $[M+2H]^{2+}$ peak of 522 Da, further supported by its unique isotopic pattern (Fig. 8d). Based on these observations, the fragmentation pattern of DP-8 was chalked out, as given in Scheme 4.

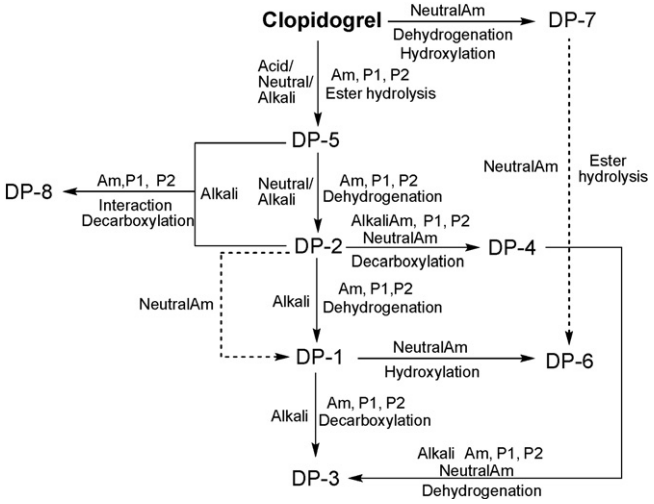

Scheme 5. Degradation pathway of clopidogrel bisulphate under solid state stress conditions. The dotted lines are for stipulated pathways.

3.8. Postulation of degradation pathway and mechanism of decomposition under solid state stress conditions

The proposed degradation pathway for the drug under various solid state stress conditions is shown in Scheme 5. It was drawn based on the structures of degradation products characterized through LC–MS studies (Schemes 1–4), considering the rise and fall of products in HPLC chromatograms with time, and possibility of mechanistic explanation.

According to it, the drug was converted to the ester hydrolytic product (DP-5), a common degradation product under solid state acid/neutral/alkali stress conditions (Fig. 3). The product was formed through a simple reaction mechanism involving ester hydrolysis. The reaction did not proceed further in acid conditions, because all other potential products of the drug involved dehydrogenation (Schemes 1–4), which was not possible in the presence of a proton donor. As shown in Fig. 9, along with small amount of hydrolytic product DP-5, peaks of DP-1 to DP-4 and DP-8 appeared in alkali condition, because of the possibility of proton abstraction. As shown in Fig. 9a, while DP-1, DP-2, DP-4 and DP-8 along with DP-5 were seen in 1 month sample, the peak heights of DP-2, DP-4 and DP-5 were reduced, and those of DP-1, DP-3 and DP-8 were increased significantly after 3 months (Fig. 9b). It was postulated that DP-5 was further converted to dehydrogenated product DP-2 by proton abstraction, catalysed by alkali microenvironment and heat. The latter was further dehydrogenated to DP-1 by the same mechanism. In the alkaline microenvironment, DP-2 was also converted to DP-4 on decarboxylation. Further, DP-2 reacted with DP-5 to form a dimeric interaction product, DP-8. It is postulated that

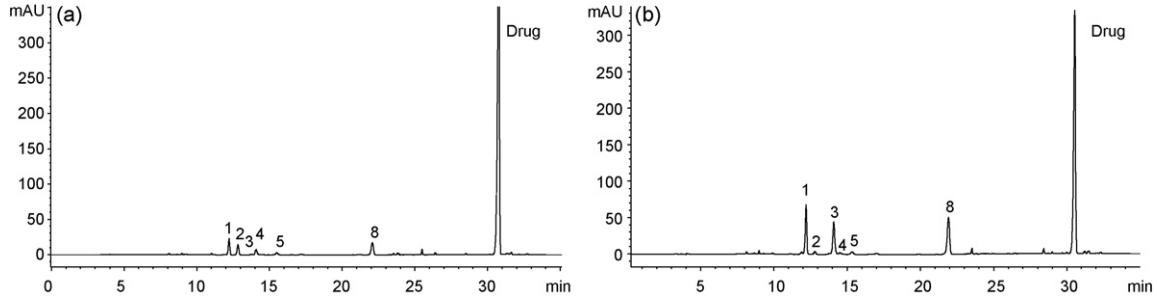

Fig. 9. Chromatogram of degradation products formed under alkali microenvironment after 1 month (a) and 3 months (b). Codes 1–5 and 8 represent DP-1 to DP-5 and DP-8, respectively.

DP-3 was formed from DP-4 and DP-1 after dehydrogenation and decarboxylation, respectively.

Among the six degradation products formed on direct exposure of the amorphous form of drug to accelerated conditions in the absence of stressors (Section 3.4.2), there were at least two new products, *viz.*, DP-6 and DP-7. It was postulated that DP-6 was produced on degradation of DP-2, with DP-1 acting as an intermediary. The product, DP-7, was formed in a similar manner from the drug by dehydrogenation and subsequent hydroxylation. Its ester hydrolysis also could result in DP-6.

The reason that similar multiple products were not observed from the amorphous form in the presence of acidic and alkaline stressors perhaps was the reduction of hygroscopicity on dilution of drug by the stressors, which was also observable through comparison of physical changes in the presence and the absence of stressors (Table 7). Similar behaviour of reduction of moisture gain on increase in bulk has been reported earlier [24].

4. Conclusion

The present study revealed that microenvironmental pH could affect both the rate and nature of degradation among different solid forms of clopidogrel bisulphate. The common decomposition mechanisms in solid state were ester hydrolysis, decarboxylation, hydroxylation, dehydrogenation and dimerization. The study indicates that an integrated approach needs to be followed to assess the stability of drugs in their solid forms.

It is hoped that characterization of the unknown degradation products of the drug will be of use to industry in setting up their limits in solid dosage forms manufactured by them.

Acknowledgement

The authors are grateful to Prof. Arvind K. Bansal, Department of Pharmaceutics, and Prof. A.K. Chakraborti, Department of Medicinal Chemistry, NIPER, for their thoughtful discussions and insightful directions.

References

[1] A.W. Newman, S.R. Byrn, Drug Discov. Today 8 (2003) 898–905.
[2] Y. Kato, M. Kohket, Chem. Pharm. Bull. 29 (1981) 268–272.
[3] N. Kimura, H. Fukui, H. Takagaki, E. Yonemochi, K. Terada, Chem. Pharm. Bull. 49 (2001) 1321–1325.
[4] S. Miyazaki, T. Arita, R. Hori, K. Ito, Chem. Pharm. Bull. 22 (1974) 638–642.
[5] B. Rodriguez-Sponga, C.P. Priceb, A. Jayasankara, A.J. Matzgerb, N. Rodriguez-Hornedoa, Adv. Drug Deliv. Rev. 56 (2004) 241–274.
[6] S.R. Byrn, J. Pharm. Sci. 65 (1976) 1–22.
[7] K. Florey, Analytical Profiles of Drug Substances, vol. 17, Academic Press, New Jersey, 1988, pp. 1–39.
[8] H.H. Tonnesen, The Photostability of Drugs and Drug Formulations, 2nd ed., Taylor & Francis, London, 2004, pp. 354–355.
[9] S.R. Byrn, W. Xub, A.W. Newman, Adv. Drug Deliv. Rev. 48 (2001) 115–136.
[10] V. Koradia, G. Chawla, A.K. Bansal, Acta Pharm. 54 (2004) 193–204.
[11] B.B. Lohray, V.B. Lohray, B. Pande, M.G. Dave, Nixon & Vanderhye, Patent US 0,037,842 (2007).
[12] P.B. Reddy, K. Reddy, R.R. Reddy, M.D. Reddy, Hetero drugs limited, Patent US 0,100,231 A1 (2006).
[13] D. Rao, Cipla Limited, Patent WO 026879 A1 (2004).
[14] A. Mitakos, I. Panderi, J. Pharm. Biomed. Anal. 28 (2002) 431–438.
[15] A. Mohan, M. Hariharan, E. Vikraman, G. Subbaiah, B.R. Venkataraman, D. Saravanan, J. Pharm. Biomed. Anal. 47 (2008) 183–189.
[16] H. Agrawal, N. Kaul, A.R. Paradkar, K.R. Mahadik, Talanta 61 (2003) 581–589.
[17] H.E. Zaazaa, S.S. Abbas, M. Abdelkawy, M.M. Abdelrahman, Talanta 78 (2009) 874–884.
[18] T.M. Serajuddin, A.B. Thakur, R.N. Ghoshal, M.G. Fakes, S.A. Ranadive, K.R. Morris, S.A. Varia, J. Pharm. Sci. 88 (1999) 696–704.
[19] R. Lifshitz, E. Kovalevski-Ishai, S. Wizel, S.A. Maydan, R. Lidor-hadas, Teva Pharmaceutical Industries Ltd., Patent US 6,767,913 B2 (2004).
[20] R. Lifshitz-Liron, E. Kovalevski, S. Wizel, S. Avhar-Maydan, R. Lidor-Hadas, Teva Pharmaceutical Industries Ltd., Patent US 7,074,928 B2 (2006).
[21] W. Danikiewiczl, M. Swist, J. Mass Spectrom. 42 (2007) 405–406.
[22] United States Pharmacopeia, 29th ed., The United States Pharmacopeial Convention, Rockville, Maryland, USA, 2006, p. 562.
[23] S.S. Singh, K. Sharma, D. Barot, P.R. Mohan, V.B. Lohray, J. Chromatogr. B 821 (2005) 173–180.
[24] S. Singh, H. Bhutani, T.T. Mariappan, H. Kaur, M. Bajaj, S.P. Pakhale, Int. J. Pharm. 245 (2002) 37–44.